

The energy recovery circuit is arranged so that clamp capacitor C5 is discharged during the on time of the primary switches. With this arrangement, the energy stored in C5 is delivered directly to the output. Zero voltage and current switching of switch S1 can be achieved if S1 is turned on when clamp diode D3 is in conduction, since the voltage across S1 is discharged to negative one diode drop and the current in T2 is slightly negative.

If it is assumed that the voltage on C5 is larger than the ideal transformer secondary voltage (V_{SEC}) and that D1 is conducting, then the voltage difference is applied across the primary of flyback transformer T2 via S1. The current in the primary of T2 increases linearly, for sufficiently large values of C5, and flows to the output via the loop formed by C5, C_{OUT} (R_{LOAD}), L_{OUT} , T2 primary and S1.

At the turn off of S1, which is timed to coincide with the turn off of the primary switches, the energy stored in the flyback transformer T2 is transferred to the output via D6. The net effect of the energy recycling circuit is to reduce the current flowing in the forward diode as the energy is drawn from clamp capacitor C5. Figure 2 shows the basic waveforms of the improved active clamp.

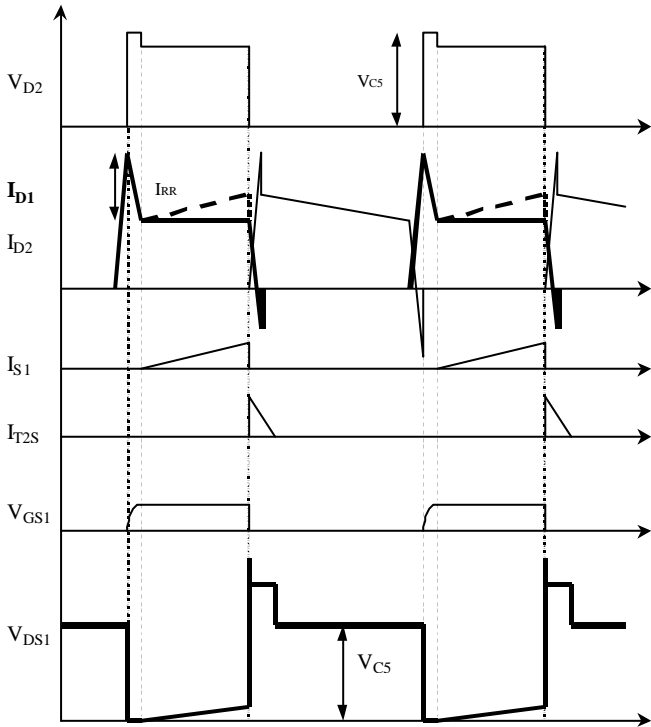


Figure 2. Basic waveforms of improved secondary active clamp

The action of clamping the voltage across converter diodes provides the major benefit of allowing diodes with lower breakdown voltages to be used, which usually have lower conduction and switching losses, and smaller reverse recovery phenomena. The benefit comes at a cost: during the action of clamping, energy from the primary circuit is transferred to the clamp in addition to the energy stored in the

leakage inductance, as shown in the equations below. In some cases, the extra energy from the primary circuit can be more than ten times the actual energy stored in the leakage inductance. As a result, the recovery of the energy stored in the clamp must be very efficient if any improvement in overall efficiency is to be obtained.

2.1 Energy Equations

During clamping of the freewheel diode, energy dumped into the clamp capacitor C5 can be derived from the integration of the capacitor current (charge) and is given by:

$$E_{C5}(in) = \left[\frac{V_{C5}}{V_{C5} - V_{SEC}} \right] \frac{L_{leak} I_{RR}^2}{2} \quad (1)$$

where V_{C5} is the voltage on clamp capacitor C5, V_{SEC} is the ideal secondary winding voltage, L_{leak} is the transformer secondary leakage inductance and I_{RR} is the amplitude of the freewheel diode reverse recovery current.

At the beginning of clamping, the energy stored in the leakage inductance is given by:

$$E_{leakage} = \frac{L_{leak} I_{RR}^2}{2} + L_{leak} I_{RR} I_{OUT} \quad (2)$$

where I_{OUT} is the output load current. Note that the second term of equation (2) can be shown to be energy being transferred from the primary to the output choke.

Once clamping is complete and S1 begins to conduct forward current, the energy drawn out of the clamp capacitor is:

$$E_{C5}(out) = \left[\frac{V_{C5}}{V_{C5} - V_{SEC}} \right] \frac{L_{T2P} I_{S1pk}^2}{2} \quad (3)$$

where L_{T2P} is the primary winding inductance of the flyback transformer and I_{S1pk} is the peak current flowing in S1 prior to the turn off of S1.

The energy delivered to the output from the secondary of the flyback transformer is given by:

$$E_{FB}(out) = \frac{L_{T2P} I_{S1pk}^2}{2} \quad (4)$$

From an analysis of the energy equations, the following conclusions can be drawn. The clamp voltage V_{C5} , is independent of the load current I_{OUT} ; proportional to the amplitude of the diode reverse recovery current I_{RR} ; inversely proportional to the on time of S1, and proportional to the square-root of the primary inductance of flyback transformer T2 if the leakage inductance of the power transformer is relatively small.

Secondly, the higher the reverse recovery current of the secondary diode is, the more useful the active clamp is in allowing an increase in switching frequency. However, the best performance is still obtained by using diodes with the lowest reverse recovery. Since the reverse recovery current spike causes increased heating in the transformer and primary power devices, it would be advantageous to have a diode with a higher forward drop and negligible reverse recovery as it is generally easier to heatsink a diode than PCB tracks or a transformer winding. The current limitations of diode technology prevent yields of negligible recovery, low conduction loss diodes since peak reverse recovery current is traded for forward voltage drop.

In addition, the energy transferred to the clamp from the primary is:

$$E_{C5}(prim) = \left[\frac{V_{C5}}{V_{C5} - V_{SEC}} - 1 \right] \frac{L_{leak} I_{RR}^2}{2} \quad (5)$$

Hence, where the clamp voltage, V_{C5} , is tightly controlled, for example, to be 105% of the ideal transformer secondary voltage, V_{SEC} , the energy transferred from the primary to the clamp capacitor is twenty times the energy stored in the leakage inductance. This means that the clamp handles a significant portion of the total converter power through another stage of conversion. As a result, the operating clamp voltage must be optimised to maximize efficiency.

3 EMC improvement considerations

Increasing switching frequencies above 150kHz means the attenuation of the fundamental component of the switching waveforms must be typically 100dB in order to meet Class B emissions for EN55022. In most cases, the differential mode voltages at the input and output capacitors of the power converter are typically more than 60dB lower than the switching voltages and can be easily lowered to meet the emission requirements. The common mode voltages are usually the source that requires the most attention to meet the Class B limits.

Common mode voltages are generated by the arrangement of the circuit components with respect to the chassis earth. For a circuit with a balanced primary power circuit, such as a double-ended forward or full bridge, there is little or no conversion of the primary side differential switching voltages to common mode voltage through the transformer winding capacitance. Secondly, if the semiconductors are mounted on a heatsink connected to the negative primary supply rail; there is no common mode current injection into the chassis. The source of common mode voltage then becomes the transformer secondary to primary voltage distribution, which depends on the transformer winding geometry and the arrangement of the secondary circuit.

In the case of a forward converter secondary, the transformer secondary to primary voltage distribution is

unbalanced and is the dominant common mode source. If the output choke is used in the positive lead and the output negative line is connected to chassis via a large capacitor, as shown in Figure 3, the full secondary voltage becomes the driving voltage for the common mode signal. The signal source and coupling can be modeled, to a first approximation, as the secondary voltage being capacitively coupled to the center tap of the primary winding. For a balanced primary, this can be simplified to a coupling directly to the primary supply rails.

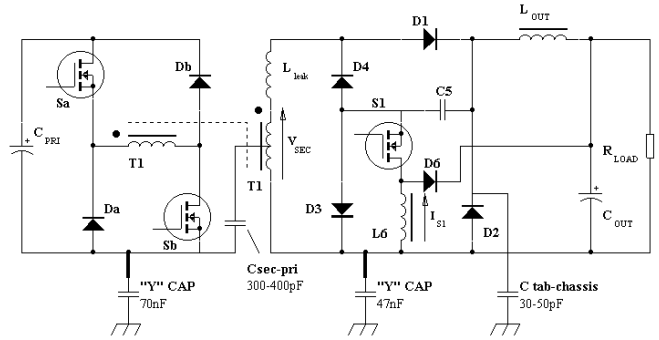


Figure 3. First stage common mode attenuation and parasitic elements for forward converter with output choke in positive leg.

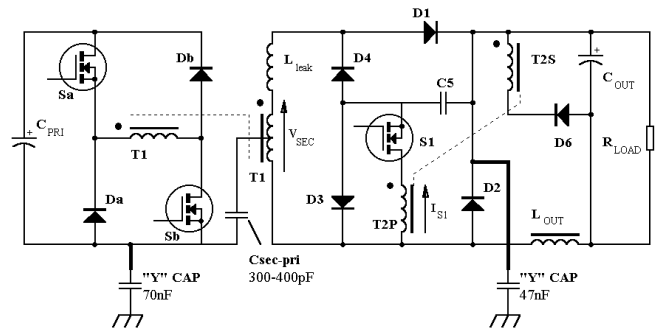


Figure 4. First stage common mode attenuation with output choke in negative output leg.

Adding "Y" capacitors to the negative rail, either directly or indirectly via the input diode bridge, then provides a degree of attenuation due to the capacitor voltage divider formed by the transformer secondary to primary winding capacitance and the total "Y" capacitance. Further attenuation is then provided on the AC line in the form of a common mode choke. To maximize the first stage attenuation, the transformer primary to secondary capacitance needs to be minimized, which usually results in a higher leakage inductance as the windings need to be moved apart. This is particularly noticeable with planar transformers where the capacitance is large if a low leakage inductance is to be obtained.

A secondary common mode source is the capacitive coupling of the cathode mounting plates (tabs) of the output diodes to the chassis if the chassis is being used as the heatsink. The voltage waveform is different to that produced

by the transformer and can be the dominant source for RF noise on the output when the diodes snap off. The output DC lines commonly use a small common mode choke to reduce output terminal common mode voltages which can couple back to the input lines and increase AC line emissions.

By moving the output choke to the negative output line, the cathodes of the output diodes can be connected to chassis by a large capacitor, as shown in Figure 4. This eliminates the common mode switching voltage from the output diodes and reduces the source voltage on the secondary by 6-10dB. The isolated winding of the secondary active clamp permits this technique in noise reduction to be used without compromising the performance of the active clamp.

4 Experimental Results

A 700W, 200kHz compact 48V rectifier was built using the improvements to the secondary active clamp and tested to verify the principle of operation, power loss saving and reduction of common mode voltage signals. Figure 5 shows the experimental secondary circuit with the component values used.

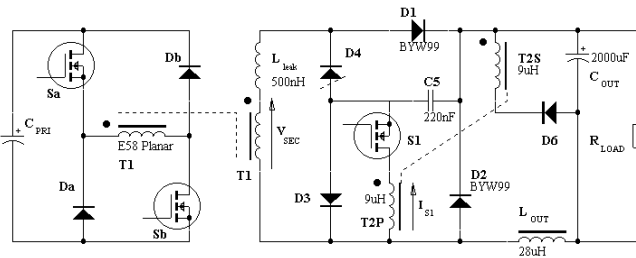


Figure 5. Experimental active clamp circuit values

Figure 6 shows the operational waveforms of the active clamp under full load, indicating the freewheel diode voltage, MOSFET drain-source voltage and drain current. From the waveforms, it is clear that the turn on of the active clamp MOSFET is made under ZVS/ZCS conditions.

Table 1 lists the results for energy recovered with various arrangements for snubbing and clamping of the secondary diodes.

The common mode driving voltage waveform for the circuit arrangement of Figure 5 with a 47nF capacitor between the output diode cathodes and chassis, is shown in Figure 7. Plots of the common mode voltage spectrum on the primary side negative rail and input terminals are shown in Figures 8 and 9 respectively. The plot of Figure 9 also shows the conducted emission limits for EN55022 Class B.

Figure 10 shows a photo of the prototype rectifier indicating the planar transformer mounted in a “minimum footprint” configuration and the primary heatsink, which is connected to the negative rail.

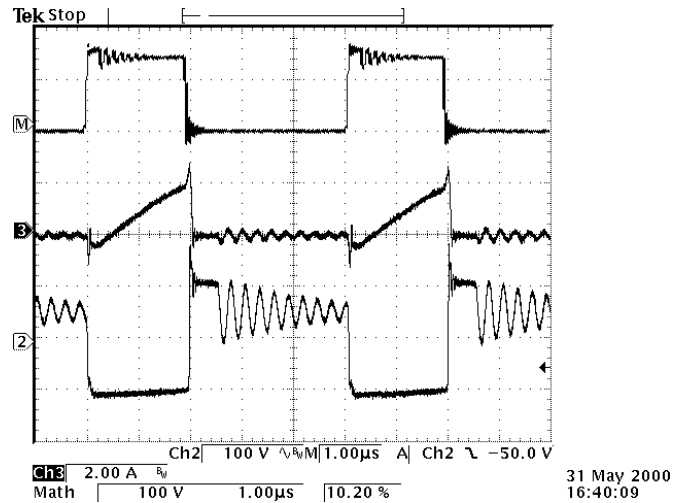


Figure 6. Operational waveforms of active clamp. (Top) freewheel diode voltage: 100V/div, (mid) active clamp MOSFET drain current: 2A/div, (bot) MOSFET drain-source voltage 100V/div (zero on -3 div).

Configuration	Reduction in Loss
400V Epitaxial Diode, RC snubber, under damped	0W
2x100V Schottky, RC snubber, underdamped (lower reverse recovery)	3W
200V Epitaxial Diode, Active Clamp	12W

Table 1. Summary of Results for various practical arrangements of secondary diodes and snubbers

5 Conclusion

Improvements to the previously reported secondary active clamp has been presented which recycles reverse recovery energy stored in the transformer leakage inductance directly to the output during the on time of the primary switches. ZVS/ZCS of the active clamp MOSFET was shown to occur if the MOSFET was turned on during clamping of the secondary diodes. Operation of the improvements were verified experimentally on a compact 700W rectifier using a planar transformer with a secondary leakage inductance of 500nH. An improvement of approximately 1.5% in converter efficiency was measured with respect to a typical RC snubber on 400V output diodes.

The magnitude of transformer primary to secondary winding capacitance was shown to directly affect the converter common mode noise, which is reduced by 6-10dB by connecting the output choke of a forward converter in the negative output leg. Through the use of an isolated winding in the energy recovery circuit, the connection of the output choke in the negative leg was permitted without compromising the performance of the active clamp.

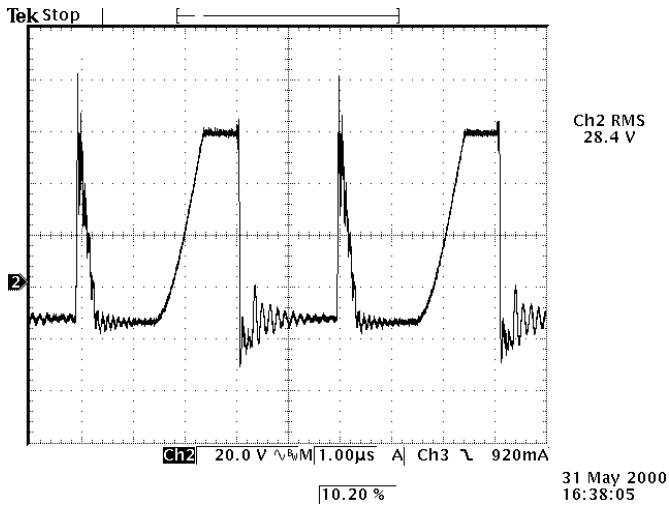


Figure 7. Common mode driving voltage appearing on transformer mid point. 20V/div.

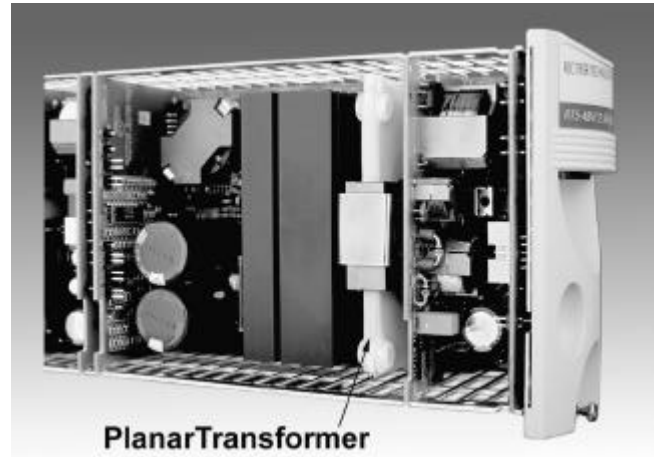


Figure 10. Photo of prototype rectifier with minimal footprint planar transformer located to the right of the primary heatsink.

6 References

- [1] J-P. Schauwers, C. Nunes, B. Velaerts, "Planar Transformer Technology Applied to AC/DC Conversion", Proc. Intelec, 1999, Copenhagen. Paper 23-3.
- [2] J. A. Sabate, et. al., "Design Considerations for High-voltage, High Power, Full-bridge, Zero-voltage-switched, PWM converter", IEEE APEC Records 1990. pp. 263-268.
- [3] A. J. Forsyth, "Review of Resonant Techniques in Power Electronic Systems", IEE Power Engineering Journal, 1996, Vol. 10, No. 3, pp 110-120.
- [4] A. I. Pressman, *Switching Power Supply Design*, McGraw-Hill, New York 1991.
- [5] K. Matsui, et. al., "Utility-interactive Photovoltaic Power Conditioning System with Forward Converter for Domestic Applications", IEE Proc. Elect. Power Appl., Vol. 147, No.3, May 2000, pp 199-205.
- [6] P. C. Todd, "Snubber Circuits: Theory, Design and Application", Unitorde Switching Regulated Power Supply Design Seminar Manual, SEM-900. Unitorde 1993.
- [7] H. Mao and M. Jacobs, "Active Snubbers to Eliminate Diode Reverse Recovery and Achieve Zero-Current Turn-Off in DC-DC Converters", Proc. Intelec, 1998, San Francisco. Paper 2-4.
- [8] J. W. Baek, C. Y. Jung, et. al., "Novel Zero-Voltage and Zero-Current-Switching (ZVZCS) Full Bridge PWM Converter with Low Output Ripple", Proc. Intelec, 1997, Melbourne. Paper 13-2.
- [9] J. Dekter, N. Machin and R. Sheehy, "Lossless Active Clamp for Secondary Circuits", Proc. Intelec, 1998, San Francisco. Paper 17-1.

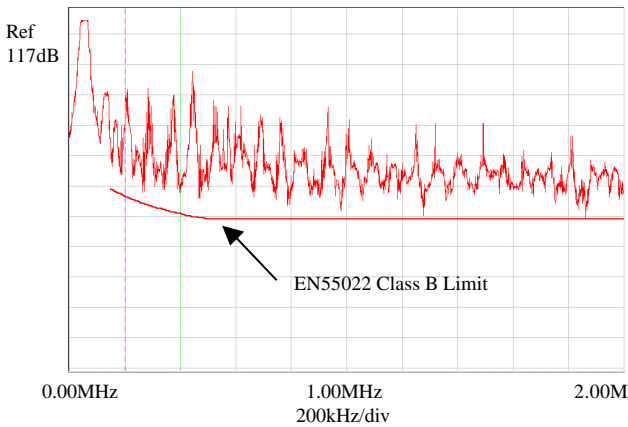


Figure 8. Common mode voltage spectrum on primary supply rail. 10dB/div

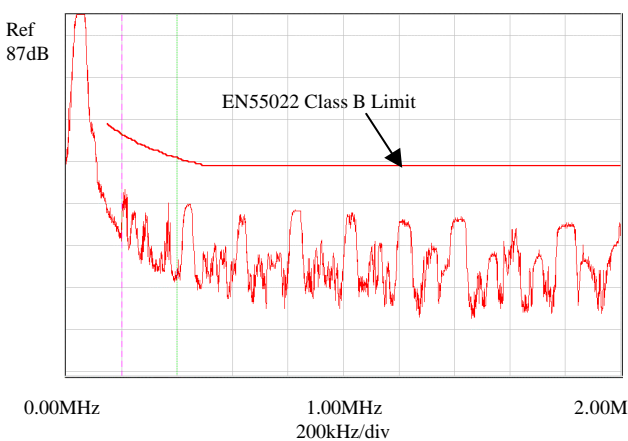


Figure 9. Common mode voltage spectrum at input terminals. 10dB/div